減）および手術待機期間の短縮を図ることができる

安全性臨床試験への展開が期待される。

E. 結論

今後の第1相安全性確認臨床試験、第2相有効性

研究成果の刊行に関する一覧

書籍

著者氏名	論文タイトル名	書籍全体の編集者名	書　籍　名	出版社名	出版地	出版年	ページ
竹原有史 松原弘明	Cardiosphereによる心筋再生	山口　徹 高本真一 中澤　誠 小室一成	Annual Review 循環器2009	中外医学社	東京	2009	p 10-17
足立淳郎 松原弘明	心不全への再生医療	北風政史	心不全診療 Skill up マニュアル	羊土社	東京	2008	p 262-269
王　英正 松原弘明	心臓内幹細胞の特性と自己複製制御機構	山中伸弥 中内啓光	再生医療へ進む最先端の幹細胞研究	羊土社	東京	2008	p 100-106
中村英夫 松原弘明	虚血性心疾患の再生治療（細胞治療）	森下竜一	血管の再生	真興交易	東京	2008	p 132-142
辰巳哲也 松原弘明	虚血性心疾患に対する再生医療	山口　徹 堀　正二	循環器疾患最新の治療	南江堂	東京	2006	p 15-20
辰巳哲也 松原弘明	血管新生療法	松尾　汎	血管疾患を知る	メジカルビュー社	東京	2005	pp184-187
松原弘明	末梢性動脈疾患（閉塞性動脈硬化症、バージャー病）	山口　徹 北原光夫	今日の治療指針	医学書院	東京	2005	299-300
辰巳哲也 高橋知三郎 王　英正 松原弘明	細胞移植と血管新生治療－末梢血管病から心臓病へ－	野出孝一	血管不全フロンティア	メディカルレビュー社	東京	2004	pp349-356
松原弘明	血管再生医療の実施と展望－骨髄系体細胞移植を用いた末梢性血管疾患・狭心症への血管新生医療－	日本老年医学会雑誌編集委員会	老年医学update 2004-2005	メジカルビュー社	東京	2004	pp156-164
辰巳哲也 松原弘明	虚血性心臓病への骨髄細胞移植による再生医療	矢崎義雄 山口　徹 高本眞一 中澤　誠	Annual Review 循環器	中外医学社	東京	2004	pp147-151

雑誌 （松原 弘明）

発表者氏名	論文タイトル名	発表誌名	巻号	ページ	出版年
Takehara N,Matsubara H ,Oh H. （他7人）	Controlled Delivery of Basic Fibroblast Growth Factor Promotes Human Cardiosphere-Derived Cell Engraftment to Enhance Cardiac Repair for Chronic Myocardial Infarction.	**J Am Coll Cardiol**	52	1858-1865	2008
Asada S, Matsubara H、Oh H. （他6人）	Downregulation of Dicer expression by serum withdrawal sensitizes human endothelial cells to apoptosis.	**Am J Physiol Heart Cire Physiol**	295	2512-2521	2008
Tagawa M, Matsubara H、Oh H. （他6人）	MURC,a muscle-restricted coiled-coil potein,is involved in the regulation of skeletal myogenesis.	**Am J PhysiolCell Physiol**	295	C490-C498	2008
Harada K, Matsubara H, Oh H. （他5人）	Crossveinless-2 controls bone morphogenetic protein signaling during early cardiomyocyte differentiation in p19cells.	**J Biol Chem**	283	26705-26713	2008
Ogata T, Matsubara H, Oh H. （他6人）	MURC, a Muscle-Restricted Coiled-Coil Protein That Modulates the Rho/ROCK Pathway, Induces Cardiac Dysfunction and Conduction Disturbance.	**Mol Cell Biol**	28	3424-3436	2008
Matsui A, Matsubara H （他10人、最終著者）	Central role of calcium-dependent tyrosine kinase PYK2 in endothelial nitric oxide synthase-mediated angiogenic response and vascular function.	**Circulation**	116	1041-1051,	2007
Takahashi T, Matsubara H.	New targeted angiogenic strategy: bursting bubbles.	**Circ Res**	101	232-233	2007
Kitamura R, Matsubara H (他8人、最終著者)	Stage-specific role of endogenous Smad2 activation in cardiomyogenesis of embryonic stem cells.	**Circ Res**	101	78-87	2007

Ogata T, **Matsubara H,** (他6人、8番目著者)	Osteopontin is a myosphere-derived secretory molecule that promotes angiogenic progenitor cell proliferation through the phosphoinositide 3-kinase/Akt pathway.	**BBRC**	359	341-347	2007
Tateishi K, **Matsubara H,** Oh H (他8人、10番目著者)	Clonally amplified cardiac stem cells are regulated by Sca-1 signaling for efficient cardiovascular regeneration	**J Cell Sci.**	120	1791-1800	2007
Yamamoto T, **Matsubara H** (他6人、最終著者)	Enhanced activity of ventricular Na+-HCO3-cotransport in pressure overload hypetrophy.	**Am J Physiol Heart Circ Physiol**	293	H1254-1264	2007
Tateishi K, **Matsubara H,** Oh H (他8人、10番目著者)	Human cardiac stem cells exhibit mesenchymal features and are maintained through Akt/GSK-3betasignaling.	**BBRC**	352	635-641	2007
Nomura T, **Matsubara H,** Oh H (他5人、7番目著者)	Skeletal myosphere-derived progenitor cell transplantation promotes neovascularization in deltasarcoglycan knockdowncardiomyopathy.	**BBRC**	352	668-674	2007
Nakajima N, **Matsubara H,** Oh H (他5人、7番目著者)	MicroRNA-1 facilitates skeletal myogenic differentiation without affecting osteoblastic and adipogenic differentiation.	**BBRC**	350	1006-1012	2007
Ikeda K, **Matsubara H** (他6人、最終著者)	Glia maturation factor-gamma is preferentially expressed in microvascular endothelial and inflammatory cells and modulates actin cytoskeleton reorganization.	**Circ Res**	99	424-433	2007
Voros S, **Matsubara H** (他6人、9番目著者)	Interaction between AT1 and AT2 receptors during postinfarction left ventricular remodeling.	**Am J Physiol Heart Circ Physiol.**	290	H1004--10	2006
Zen K **Matsubara H** (他9人、最終著者)	Myocarium-targeted delivery of endothelial progenitor cells by ultrasound-mediated microbubble destruction improves cardiac function via an angiogenic respone	**J Mol Cell Cardiol.**	40	799-809	2006

Urao N, **Matsubara H** (他9人、最終著者)	Erythropoietin-Mobilized Endothelial Progenitors Enhance Reendothelialization via Akt-Endothelial Nitric Oxide Synthase Activation ando Prevent Neointimal Hyperplasia	**Circ Res**	98	1405-1413	2006
Nishikawa S, **Matsubara H** (他9人、最終著者)	Nicorandil regulates Bcl-2 family proteins and protects cardiac myocytes against hypoxia-induced apoptosis.	**J Mol Cell Cardiol.**	40	510-519	2006
Matsuno K, Yamada H, Iwata K, Jin D, Katsuyama M, Matsuki M, Takai S, Yamanishi K, Miyazaki M, Matsubara H, Yabe-Nishimura C.	Nox1 is involved in angiotensin II-mediated hypertension: a study in Nox1-deficient mice.	**Circulation.**	25	2677-85	2005
Tsunoda S, Mazda O, Oda Y, Iida Y, Akabame S, Kishida T, Shin-Ya M, Asada H, Gojo S, Imanishi J, Matsubara H, Yoshikawa T.	Sonoporation using microbubble BR14 promotes pDNA/siRNA transduction to murine heart.	**Biochem Biophys Res Commun.**	14	118-27	2005
Takamiya M, Okigaki M, Jin D, Takai S, Nozawa Y, Adachi Y, Urao N, Tateishi K, Nomura T, Zen K, Ashihara E, Miyazaki M, Tatsumi T, Takahashi T, Matsubara H	Granulocyte Colony-Stimulating Factor-Mobilized Circulating c-Kit+/Flk-1+ Progenitor Cells Regenerate Endothelium and Inhibit Neointimal Hyperplasia After Vascular Injury.	**Arterioscler Thromb Vasc Biol.**	26	751-7	2006
Imada T, Tatsumi T, Mori Y, Nishiue T, Yoshida M, Masaki H, Okigaki M, Kojima H, Nozawa Y, Nishiwaki Y, Nitta N, Iwasaka T, Matsubara H.	Targeted delivery of bone marrow mononuclear cells by ultrasound destruction of microbubbles induces both angiogenesis and arteriogenesis response.	**Arterioscler Thromb Vasc Biol.**	25	2128-34	2005
Irie H, Okigaki M, Zen K, Takamiya M, Takahashi T, Azuma A, Tatsumi T, Matsubara H.	Carbon Dioxide-Rich Water Bathing Enhances Collateral Blood Flow In Ischemic Hindlimb via Mobilization of Endothelial Progenitor Cells and Activation of NO-cGMP System	**Circulation**	111	1523-29	2005

Tatsumi T, Akashi K, Keira N, Matoba S, Mano A, Shiraishi J, Yamanaka S, Kobara M, Hibino N, Hosokawa S, Asayama J, Fushiki S, Fliss H, Nakagawa M, Matsubara H..	Cytokine-induced nitric oxide inhibits mitochondrial energy production and induces myocardial dysfunction in endotoxin-treated rat hearts	**J Mol Cell Cardiol.**	37	775-84	2004
Mano A, Tatsumi T, Shiraishi J, Keira N, Nomura T, Takeda M, Nishikawa S, Yamanaka S, Matoba S, Kobara M, Tanaka H, Shirayama T, Takamatsu T, Nozawa Y, Matsubara H.	Aldosterone directly induces myocyte apoptosis through calcineurin-dependent pathways.	**Circulation**	110	317-23	2004
Amano K , Okigaki M, Adachi Y, Fujiyama S, Mori Y, Kosaki A, Iwasaka T and Matsubara H	Mechanism for IL-1β-mediated neovascularization unmasked by IL-1β knock-out mice,	**J Mol Cell Cardiol**	36	459-640	2004
Matsubara H.	Risk to the coronary arteries of intracoronary stem cell infusion and G-CSF cytokine therapy.	**Lancet.**	363	746-7	2004
Higashi Y, Kimura M, Hara K, Noma K, Jitsuiki D, Nakagawa K, Oshima T, Chayama K, Sueda T, Goto C, Matsubara H, Murohara T, Yoshizumi M.	Autologous bone-marrow mononuclear cell implantation improves endothelium-dependent vasodilation in patients with limb ischemia.	**Circulation** .	109	1215-8	2004

雑誌　（王　英正）

発表者氏名	論文タイトル名	発表誌名	巻号	ページ	出版年
Kitamura R, Oh H (他8人、8番目著者)	Stage-specific role of endogenous Smad2 activation in cardiomyogenesis of embryonic stem cells.	**Circ Res**	101	78-87	2007
Ogata T, Oh H (他6人、最終著者)	Osteopontin is a myosphere-derived secretory molecule that promotes angiogenic progenitor cell proliferation through the phosphoinositide 3-kinase/Akt pathway.	**BBRC**	359	341-347	2007

Tateishi K, Oh H (他8人、最終著者)	Clonally amplified cardiac stem cells are regulated by Sca-1 signaling for efficient cardiovascular regeneration	**J Cell Sci.**	120	1791-1800	2007
Tateishi K, Oh H (他8人、最終著者)	Human cardiac stem cells exhibit mesenchymal features and are maintained through Akt/GSK-3betasignaling.	**BBRC**	352	635-641	2007
Nomura T, Oh H (他5人、最終著者)	Skeletal myosphere-derived progenitor cell transplantation promotes neovascularization in deltasarcoglycan knockdowncardiomyopathy.	**BBRC**	352	668-674	2007
Oh H, Chi X, Bradfute SB, Mishina Y, Pocius J, Michael LH, Behringer RR, Schwartz RJ, Entman ML, Schneider MD.	Cardiac muscle plasticity in adult and embryo by heart-derived progenitor cells	**Annu. NY. Acad. Sci.**	１０１５	１８２－９	２００４
Oh H, Bradfute SB, GallardoTD, Nakamura T, Gaussin V, Mishina Y, Pocius J, Michael LH, Behringer RR, Garry DJ, Entman ML, Schneider MD..	Cardiac progenitor cells from adult myocardium: homing, differentiation, and fusion after infarction	**Proc Natl Acad Sci U S A**	１００	１２３１３－８	２００３
Oh H, Wang SC, Prahash A, Sano M, Moravec CS, Taffet GE, Michael LH, Youker KA, Entman ML, Schneider MD.	Telomere attrition and Chk2 activation in human heart failure.	**Proc Natl Acad Sci U S A.**	100	378-83	2003
Sano M, Abdellatif M, Oh H, Xie M, Bagella L, Giordano A, Michael LH, DeMayo FJ, Schneider MD.	Activation and function of cyclin T-Cdk9 (positive transcription elongation factor-b) in cardiac muscle-cell hypertrophy.	**Nat Med.**	8	1310-7	2002
Oh H, Taffet GE, Youker KA, Entman ML, Overbeek PA, Michael LH, Schneider MD.	Telomerase reverse transcriptase promotes cardiac muscle cell proliferation, hypertrophy, and survival.	**Proc Natl Acad Sci U S A.**	98	10308-13	2001

Journal of the American College of Cardiology
© 2008 by the American College of Cardiology Foundation
Published by Elsevier Inc.

Vol. 52, No. 23, 2008
ISSN 0735-1097/08/$34.00
doi:10.1016/j.jacc.2008.06.052

MINI-FOCUS: CELL-BASED THERAPY

Controlled Delivery of Basic Fibroblast Growth Factor Promotes Human Cardiosphere-Derived Cell Engraftment to Enhance Cardiac Repair for Chronic Myocardial Infarction

Naofumi Takehara, MD, PHD,* Yoshiaki Tsutsumi, MD, PHD,‖ Kento Tateishi, MD, PHD,*‖ Takehiro Ogata, MD, PHD,* Hideo Tanaka, MD, PHD,¶ Tomomi Ueyama, MD, PHD,* Tomosaburo Takahashi, MD, PHD,*‖ Tetsuro Takamatsu, MD, PHD,¶ Masanori Fukushima, MD, PHD,† Masashi Komeda, MD, PHD,§ Masaaki Yamagishi, MD, PHD,# Hitoshi Yaku, MD, PHD,# Yasuhiko Tabata, PHD, DMEDSCI, DPHARM,‡ Hiroaki Matsubara, MD, PHD,*‖ Hidemasa Oh, MD, PHD*

Kyoto and Toyohashi, Japan

Objectives This study was designed to determine whether controlled release of basic fibroblast growth factor (bFGF) might improve human cardiosphere-derived cell (hCDC) therapy in a pig model of chronic myocardial infarction.

Background Current cell therapies for cardiac repair are limited by loss of the transplanted cells and poor differentiation.

Methods We conducted 2 randomized, placebo-controlled studies in immunosuppressed pigs with anterior myocardial infarctions. Four weeks after coronary reperfusion, 14 pigs were randomly assigned to receive an intramyocardial injection of placebo medium with or without bFGF-incorporating hydrogel implantation. As a second study, 26 pigs were randomized to receive controlled release of bFGF combined with or without hCDCs or bone marrow–derived mesenchymal stem cell transplantation 4 weeks after reperfusion.

Results Controlled release of bFGF in ischemic myocardium significantly augmented the formation of microvascular networks to enhance myocardial perfusion and contractile function. When combined with cell transplantation, the additive effects of bFGF were confined to hCDC-injected animals, but were not observed in animals receiving human bone marrow–derived mesenchymal stem cell transplantation. This was shown by increased donor-cell engraftment and enhanced cardiomyocyte differentiation in the transplanted hearts, resulting in synergistically improved ventricular function and regional wall motion and reduced infarct size.

Conclusions Controlled delivery of bFGF modulates the post-ischemic microenvironment to enhance hCDC engraftment and differentiation. This novel strategy demonstrates significant functional improvements after myocardial infarction and may potentially represent a therapeutic approach to be studied in a clinical trial in human heart failure. (J Am Coll Cardiol 2008;52:1858–65) © 2008 by the American College of Cardiology Foundation

Stem cell therapies offer tremendous possibilities for curative approaches toward restoring lost myocardium and cardiac function; however, recent studies have indicated that effective cardiac muscle regeneration might be

See page 1866

hindered by poor cell engraftment and inefficient cardiomyocyte differentiation of the transplanted cells in the absence of integration with the host myocardial environment after infarction (1). Although prior studies (2–5)

From the *Department of Experimental Therapeutics, †Division of Clinical Trial Design and Management, Translational Research Center, and the ‡Department of Biomaterials, Institute for Frontier Medical Sciences, Kyoto University, Kyoto, Japan; §Department of Cardiovascular Surgery, Toyohashi Heart Center, Toyohashi, Japan; and the Departments of ‖Cardiovascular Medicine, ¶Pathology and Cell Regulation, and #Cardiovascular Surgery, Kyoto Prefectural University of Medicine, Kyoto, Japan. Supported by grants-in-aid from the Ministry of Education, Culture, Sports, Science and Technology, and by grants-in-aid from the Ministry of Health, Labor, and Welfare. Drs. Tabata and Oh have applied for patents. Drs. Takehara and Tsutsumi contributed equally to this work.

Manuscript received March 7, 2008; revised manuscript received June 4, 2008, accepted June 10, 2008.

including our report have suggested human cardiac stem/progenitor cells as an attractive cell source for cardiac repair, the beneficial effects of these cells in large animal models have yet to be investigated.

The basic fibroblast growth factor (bFGF) is a pluripotent mitogen and possesses properties to promote stem cell differentiation, proliferation, and survival (3,6,7). Biodegradable gelatin is a useful delivery modality to circumvent the short half-life of recombinant bFGF in vivo. We have designed a controlled-release system for bFGF composed of acidic gelatin, which forms a poly-ion complex with bFGF (8). Biodegradable hydrogels display excellent biocompatibility demonstrated by the absence of rejection and inflammation and achieve a controlled release of bFGF in vivo as a result of hydrogel degradation within 3 weeks (9). Controlled release of bFGF has been shown to effectively enhance neoangiogenesis in human ischemic limbs (10).

This study was conducted to test whether the cell engraftment, survival, and differentiation potential of human cardiosphere-derived cells (hCDCs) could be promoted by controlled delivery of bFGF-incorporating hydrogel in response to experimental myocardial infarction, ultimately leading to improved performance in cardiovascular regeneration.

Abbreviations and Acronyms

bFGF = basic fibroblast growth factor
DMEM = Dulbecco's Modified Eagle Medium
FISH = fluorescent in situ hybridization
hBMC = human bone marrow–derived mesenchymal stem cell
hCDC = human cardiosphere-derived cell
LV = left ventricle/ventricular
LVEF = left ventricular ejection fraction
MRI = magnetic resonance imaging
SPIO = superparamagnetic iron oxide
SRS = systolic radial strain

Methods

Isolation and expansion of hCDCs from human heart samples. Human samples were obtained from 10 male patients undergoing cardiac surgery, in conformity with the guidelines of the Kyoto University Hospital and Ministry of Education, Culture, Sports, Science, and Technology, Japan. Samples were excised, minced, and digested with 0.2% type II collagenase and 0.01% DNase I (Worthington Biochemical Corp., Lakewood, New Jersey) to obtain single cell suspensions to generate cardiospheres as described previously (3). Cardiospheres were mechanically selected from the cultures and expanded in Dulbecco's Modified Eagle Medium (DMEM)/F12 medium containing 10% fetal bovine serum, 2% penicillin and streptomycin, and 40 ng/ml human recombinant bFGF (Promega Corp., Madison, Wisconsin). Six independent human bone marrow–derived mesenchymal stem cells (hBMCs) were purchased from the RIKEN Cell Bank (RIKEN Bioresource Center, Ibaraki, Japan) (11). The hBMCs were plated in DMEM containing 10% fetal bovine serum, 2% penicillin, streptomycin, and 4 ng/ml bFGF. Cells were harvested at passage 2, frozen at −80°C, and were thawed to process the third rounds of passage 3 weeks before the transplantation. The expanded hBMCs were characterized by a fluorescence-activated cell sorter using CD29, CD105, CD71, and CD90.

Generation of gelatin hydrogel sheet. The gelatin was isolated by an alkaline process from bovine bone with an isoelectric point of 5.0 as previously described (10). The water content of gelatin hydrogel was prepared to 94% by chemical cross-linking at 140°C for 72 h. The gelatin was reinforced by polytetrafluoroethylene (W. L. Gore and Associates, Inc., Flagstaff, Arizona) pericardial sheet (12) to provide strength against the beating heart. Human recombinant bFGF (Kaken Pharmaceutical Co., Tokyo, Japan) was incorporated into the gelatin hydrogel by impregnation for 3 h before implantation.

Animal models and study protocol. Based on computer-generated random allocation, we performed 2 randomized studies of chronically instrumented animals (Fig. 1). Myocardial infarction was created in 60 female Yorkshire pigs by inflating the balloon at the left ascending coronary artery for 90 min, followed by reperfusion. Thirteen of the study pigs died in the early postoperative period. We excluded 7 pigs with an ejection fraction <35% or >45% determined by transthoracic echocardiography using the Teichholz method before randomization. Animals were assigned for randomization 1 week after the creation of myocardial infarction, and then cells were grown in culture for 3 weeks to prepare for transplantation. Four study pigs died within 1 week after randomization but before the treatment due to heart failure.

In study 1, the eligible pigs (n = 14) were randomized to receive DMEM intramyocardial injection with or without 200 μg bFGF-incorporating gelatin hydrogel implantation 4 weeks after reperfusion. In study 2, we randomly assigned eligible pigs (n = 26) to receive bFGF hydrogel sheet implantation with intramyocardial injections of either DMEM, 2.0×10^7 hBMCs, or 2.0×10^7 hCDCs. All animals in both studies were immunosuppressed with cyclosporine A (Novartis Pharmaceuticals, East Hanover, New Jersey) 5 mg/kg daily from 5 days before transplantation until the time for sacrifice (13). Transplantation was performed by a 3-ml injection at 30 different sites along the border zone and in the center of the scar area.

Fluorescence-activated cell sorter analysis. Single cell suspensions were stained with the following antibodies: phycoerythrin-conjugated antibodies against CD29, and fluorescein isothiocyanate–conjugated antibodies against CD45 (all from BD Biosciences, San Jose, California) or CD105 (Ancell, Bayport, Minnesota). Antibody against mouse anti-human CD90 was detected by phycoerythrin-conjugated gout anti-mouse immunoglobin G (BD Biosciences). Samples were analyzed by FACSCalibur flow cytometer (BD Biosciences).

Generation of retroviral vectors. The *LacZ* reporter gene was subcloned into a human cardiac troponin I promoter

JACC Vol. 52, No. 23, 2008
December 2, 2008:1858–65

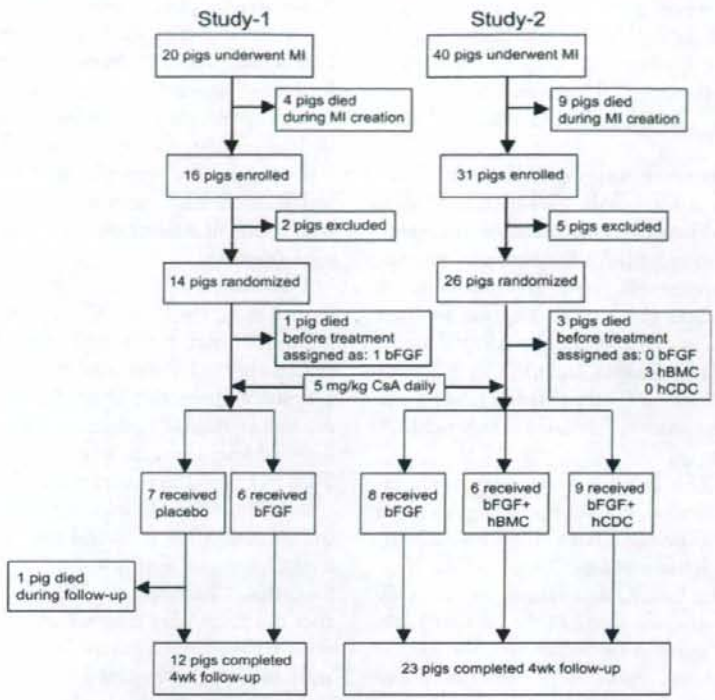

Figure 1 **Study Design**

bFGF = basic fibroblast growth factor; CsA = cyclosporine A; hBMC = human bone marrow-derived mesenchymal stem cell; hCDC = human cardiosphere-derived cell; MI = myocardial infarction.

containing plasmid (14). The hCDCs were infected by retrovirus containing pDsRed2-1 (Clontech Laboratories, Inc., Mountain View, California) and were co-cultured with neonatal rat ventricular myocytes for 4 to 5 days.

Calcium transients and electrophysiological studies. Cells were loaded with fluo-4/AM (0.625 mg/ml) and incubated with fluo-4-free Tyrode's solution at 37°C as previously described (15). Confocal images of fluo-4 and DsRed fluorescence intensities were obtained under excitation with an argon-laser and a krypton laser, respectively. The signals of action potentials from the electrodes were digitized and displayed on a digital oscilloscope (Model 310, Nicolet Instrument Technologies, Madison, Wisconsin) and stored onto a computer for offline analysis.

Immunostaining and fluorescence in situ hybridization (FISH) analysis. Paraffin-fixed sections were stained using the following primary antibodies: Cy3-conjugated mouse anti–alpha-smooth muscle actin, mouse anti-sarcomeric alpha-actin, rabbit anti-connexin 43 (all from Sigma-Aldrich, St. Louis, Missouri), mouse anti-myosin heavy chain, or rabbit anti-beta-galactosidase (all from Abcam Inc., Cambridge, Massachusetts). Secondary antibodies were conjugated to Alexa fluorochromes and nuclei were visualized using 4,6-diamino-2-phenylindole (Invitrogen Corp. [Molecular Probe], Carlsbad, California). Arteriolar density was evaluated morphometrically by histological examination of 10 randomly selected fields recognized as anti–alpha-smooth muscle actin positive structures corrected by the total area of tissue sections measured. FISH was performed as previously described (16). Deoxyribonucleic acid probes for Cy3-conjugated human Y-chromosome (classical satellite) and Cy5-conjugated porcine-specific genome were from Masahisa Tsuji (Chromosome Science Laboratory, Hiroshima, Japan). Images were captured with a BZ-8000 (Keyence, Osaka, Japan) and confocal microscope (Leica Microsystems, Wetzlar, Germany).

Reverse transcriptase polymerase chain reaction and Western blotting. Total ribonucleic acid was extracted with Trizol reagent (Invitrogen) and complementary deoxyribonucleic acid was generated using a SuperScript III complementary deoxyribonucleic acid synthesis kit (Invitrogen). Polymerase chain reactions were performed with human-specific primers as shown in the Supplemental Table. Transferred membranes were incubated with primary antibodies against phospho-Akt (S473), Akt, phospho–extracellular signal-related kinase 1/2, extracellular signal-

related kinase 1/2, phosho-p38, p38, phospho–Jun N-terminal kinase 1/2, or Jun N-terminal kinase 1/2 (all from Cell Signaling Technology Inc., Danvers, Massachusetts) as described previously (7). Horseradish peroxidase–conjugated anti-rabbit immunoglobin G was used as a secondary antibody.

Cardiac magnetic resonance imaging (MRI). MRI images were obtained on a 1.5-T MR scanner (GE Medical Systems, Milwaukee, Wisconsin) using electrocardiography-gating. Global left ventricular (LV) function was assessed using a steady-state precession pulse sequence from 8 contiguous short-axis slices (17). Infarct size was analyzed by the late-enhancement MRI technique using contrast agent (Omniscan, Daiichi-Sankyo, Japan). The LV mass was analyzed using MASS software (Medis, Leiden, the Netherlands) and infarct size was calculated as enhanced LV mass (g)/total LV mass (g).

Iron-oxide labeling. The hCDCs were magnetically labeled before injection by using a superparamagnetic iron oxide (SPIO) (Nihon Schering, Osaka, Japan) with hemagglutinating virus of Japan envelope (GenomONE Neo) (Ishihara Sangyo Kaisha Ltd., Osaka, Japan). Magnetically labeled hCDCs were assessed from 14 to 18 contiguous short-axis images by using pulse parameters for cardiac gated, fast gradient-recoiled echocardiography. The SPIO-labeled areas were measured and corrected by the values of SPIO densities of interest (18).

Echocardiography. Echocardiography was performed using a Vivid 7 Echocardiography System (GE Vingmed Ultrasound, Horten, Norway) with a M3S transducer. Real-time myocardial contrast echocardiography was performed by intravenous infusion of Levovist (Nihon, Schering) as previously described (19). Equal-sized transmural regions of interest were placed in the ischemic border area and nonischemic posterolateral wall. Signal intensities in each region of interest were assessed 3 times and the ratios were calculated.

Two-dimensional strain echocardiography was performed using the EchoPAC program (GE Vingmed). The ischemic region, border area, and nonischemic posterolateral area of the LV were analyzed at medial and apical levels as described previously (20). The LV wall motion index was defined as the ratio of peak systolic radial strain (SRS); [(medial level ischemic area SRS/medial level control area SRS) + (medial level border area SRS/medial level control area SRS) + (apical level ischemic area SRS/apical level control area SRS) + (apical level border area SRS/apical level control area SRS)]/4.

Statistics. Changes in variables from baseline to 4 weeks after treatment were analyzed with the paired *t* test. Differences between any 2 groups from baseline to 4 weeks were assessed with the Student *t* test using JMP software (SAS Institute, Cary, North Carolina). A value of $p < 0.05$ was regarded as statistically significant.

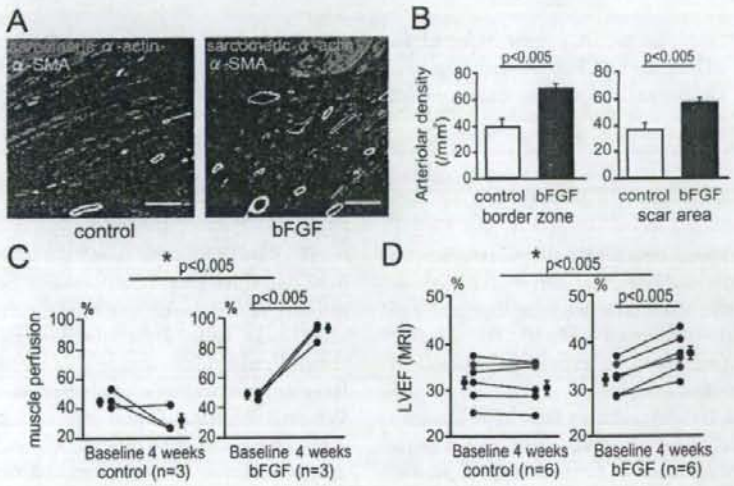

Figure 2 **Controlled Delivery of bFGF Promotes Neoangiogenesis and Restores Cardiac Function in Ischemic Myocardium**

(A and B) Arteriolar density was measured by alpha-SMA staining in control and bFGF-treated hearts (n = 6). **Bars** = 50 μm **(A). (C)** Myocardial perfusion was measured by myocardial contrast echocardiography. Signal intensities in the ischemic zone corrected by control area are shown. **(D)** Functional recovery with bFGF treatment MI analyzed by magnetic resonance imaging. **Asterisks** indicate the comparisons of absolute change in respective measurement from baseline to 4 weeks follow-up in control and bFGF-treated groups. SMA = smooth muscle actin; other abbreviations as in Figure 1.

JACC Vol. 52, No. 23, 2008
December 2, 2008:1858–65

Results

Randomized, placebo-controlled trial 1: controlled delivery of bFGF enhances myocardial perfusion and restores cardiac function in ischemic myocardium. Immunosuppressed pigs were randomized to receive intramyocardial injection of culture medium with or without bFGF-incorporating gelatin hydrogel implantation 4 weeks after myocardial infarction. A significant increase in the formation of arterial vessels was found in both infarct border zones ($66.5 \pm 5.8/mm^2$ vs. $38.6 \pm 5.8/mm^2$; $p < 0.005$) and necrotic areas ($56.9 \pm 4.2/mm^2$ vs. $36.9 \pm 4.3/mm^2$; $p < 0.005$) as compared with control hearts (Figs. 2A and 2B). Myocardial contrast echocardiography showed that bFGF-treated animals exhibited remarkably enhanced myocardial perfusion when compared with myocardial perfusion of the control group at 4 weeks ($89.7 \pm 5.9\%$ vs. $26.3 \pm 0.6\%$, $p < 0.005$) (Fig. 2C). In addition, bFGF significantly improved left ventricular ejection fraction (LVEF) at 4 weeks (LVEF: $37.1 \pm 4.2\%$ vs. $31.8 \pm 4.7\%$; $p < 0.005$). The absolute change in LVEF from baseline to 4 weeks was significantly greater in the pigs treated by bFGF compared with the change in the LVEF of the control group ($+4.9 \pm 0.5\%$ vs. $-0.4 \pm 0.4\%$; $p < 0.005$) (Fig. 2D).

Placebo-controlled trial: bFGF increases hCDC engraftment. As a preliminary experiment to confirm the beneficial effects of bFGF on hCDCs, we conducted a placebo-controlled study to compare engraftment efficiency of hCDC transplantation with or without controlled release of bFGF using SPIO nanoparticles to track hCDCs in vivo. The morphological, surface marker, stem cell transcription factor expression, calcium flux, and single cell electrical data indicate that the hCDCs that we cultured were the same cells described in previous studies (Online Fig. 1) (3,4). At 4 weeks after implantation, there was a significant retention of transplanted hCDCs in the ischemic myocardium when combined with bFGF treatment compared with hCDC injection alone (Figs. 3A and 3B). Absolute changes in LVEF and infarct volume were both synergistically improved in hCDC transplantation with bFGF than in hCDC injection alone at 4 weeks after implantation (Figs. 3C and 3D).

Randomized, placebo-controlled trial 2: epicardial delivery of bFGF with cell therapy improves cardiac function. We next performed a second, randomized study to determine whether the combination of bFGF with stem cell therapy could improve cardiac function further after chronic

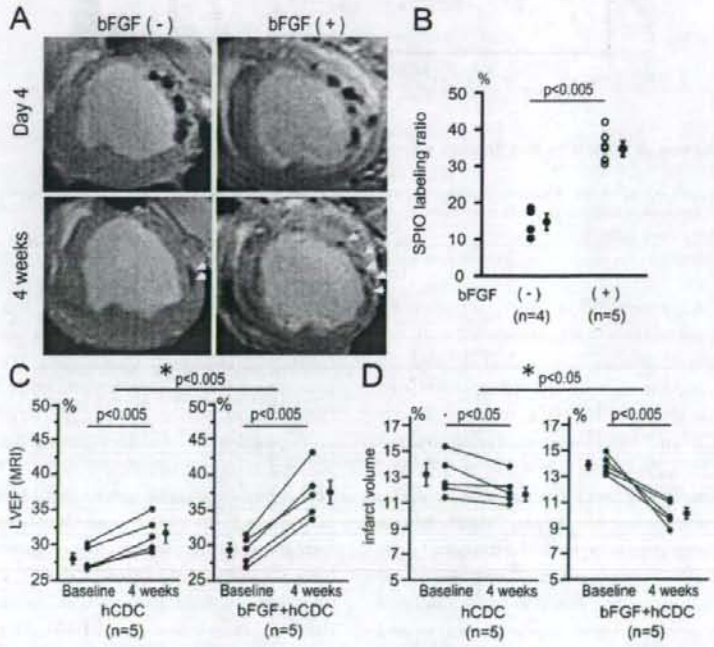

Figure 3 The Impact of bFGF on hCDCs In Vivo

(A) Paired MRIs were examined at day 4 and 4 weeks after hCDC transplantation with or without bFGF treatment. The low intensity of SPIO-labeled area is shown by **yellow arrowheads**. **(B)** Cell engraftment was estimated by the retention of SPIO-labeled cells at 4 weeks corrected by that at day 4. **(C)** Functional recovery of hCDC transplantation with or without bFGF analyzed by MRI. **(D)** Infarct size was evaluated and compared before and after treatment. **Asterisks** indicate the comparisons of absolute change in respective measurement from baseline to 4 weeks' follow-up in control and bFGF-treated groups. LVEF = left ventricular ejection fraction; MRI = magnetic resonance imaging; SPIO = superparamagnetic iron oxide; other abbreviations as in Figure 1.

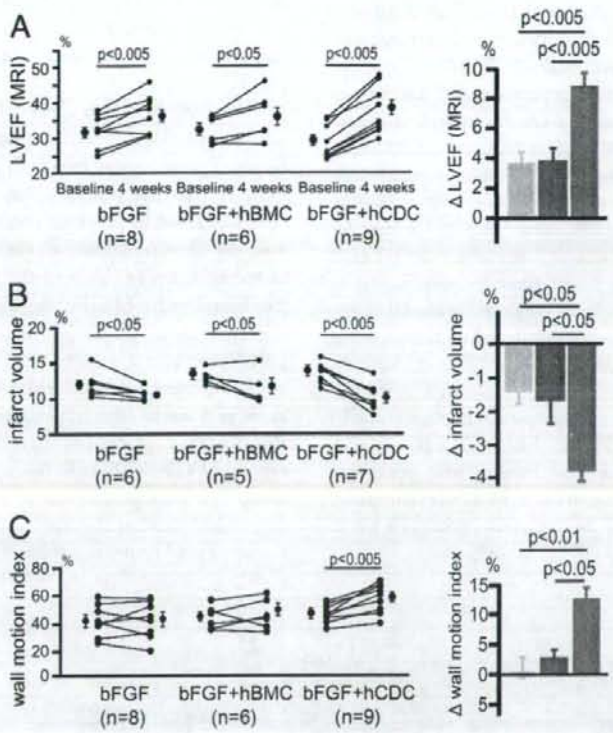

Figure 4 **Controlled Delivery of bFGF With Cell Therapy Improves Cardiac Function**

(A and B) The LVEF and infarct size at baseline and 4 weeks after treatment was measured by MRI. **(C)** The wall motion index was assessed by 2-dimensional strain echocardiography. Absolute change in each measurement was summarized and is shown on the **right. Green bars** = bFGF; **pink bars** = bFGF+hBMC; **red bars** = bFGF+hCDC. Abbreviations as in Figures 1 and 3.

myocardial infarction. Although bFGF alone significantly improved LVEF and reduced infarct size compared with the baseline, transplantation of hBMCs with bFGF had no additive effects on cardiac function (Figs. 4A and 4B). In contrast to the negligible effects of hBMCs, ischemic hearts implanted with hCDCs and bFGF-incorporating hydrogels, both LVEF (38.4 ± 6.2% vs. 30.1 ± 4.3%, $p < 0.005$) and regional wall motion (58.5 ± 11.7% vs. 46.2 ± 7.2%, $p < 0.005$) showed significant improvements; infarct volume was also remarkably reduced compared with the baseline (Figs. 4A to 4C). The magnitude of improvement after transplantation of hCDCs with bFGF in cardiac function and infarct size are significantly evident compared with cardiac function and infarct size of the control group by a comprehensive analysis of both studies 1 and 2 (Online Fig. 2).

Effects of controlled release of bFGF on cardiac regeneration after cell transplantation. To assess if cardiac function was restored, at least in part, by cardiomyocyte differentiation from the transplanted cells, we engineered 3 independent hCDCs to express a *LacZ* reporter gene under the control of human cardiac troponin-I promoter (cTnI-LacZ) by retrovirus infection (14). Immunofluorescence analyses in hCDC transplants showed that beta-gal-expressing cells were co-localized with myosin heavy chain and sarcomeric alpha-actin and were functionally coupled in the ischemic border zone (Figs. 5A to 5D).

We performed FISH experiments to identify the transplanted human male donor cells in female recipients (Fig. 5E). The functional improvement observed in hCDC transplantation with bFGF was confirmed by a greater magnitude of myocyte conversion compared with the injection of hBMCs combined with bFGF (Figs. 5F to 5H). Although myocyte regeneration was almost exclusively (>90%) through cell fusion in hBMC transplants with bFGF treatment, approximately 33% of the differentiated human cardiomyocytes were independent from cell fusion in hCDC injection with bFGF (Fig. 5H).

Discussion

Successful cell engraftment is a critical component to achieve a significant improvement in LVEF for long-term

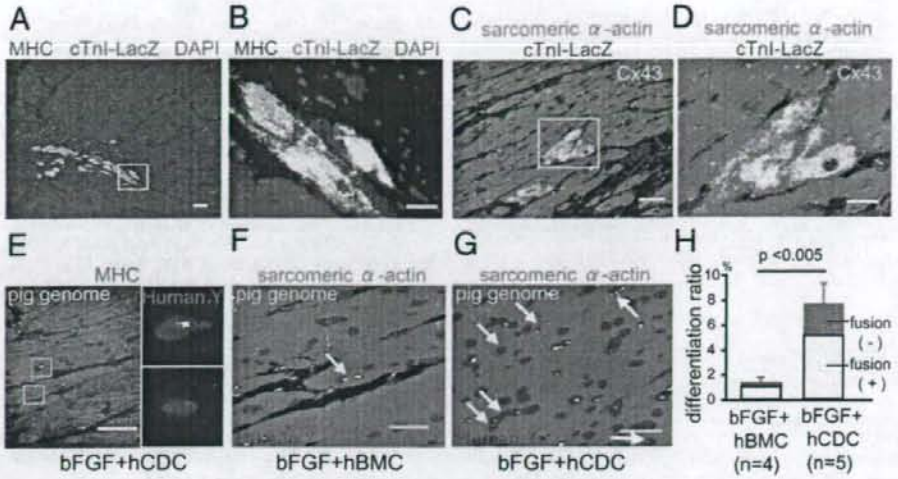

Figure 5 **Myocardial Repair by Combination of bFGF and Cell Transplantation**

(A) Differentiated cardiomyocytes expressing beta-gal **(green)** were counterstained with MHC **(red)**. **(B)** Magnified image is shown. **(C and D)** Differentiated human cardiomyocytes expressed connexin 43 **(yellow)** and sarcomeric alpha-actin **(green)**. **(E)** The FISH analysis. In hCDC transplantation, hCDCs **(red)** differentiated into human cardiomyocytes **(light blue)** with pig genome sequences **(white)** suggesting cell fusion **(upper inset)**. Autonomous differentiation is shown by hCDC-derived human cardiomyocytes lacking pig genome sequences **(lower inset)**. **(F and G)** Myocyte regeneration with **(white arrows)** or without **(yellow arrows)** cell fusion events is shown. **(H)** Quantitative analysis of cardiomyocyte regeneration and fusion. Human Y chromosome and sarcomeric alpha-actin–positive cells were counted and corrected by the total number of myocytes analyzed (>15,000 cells). The DAPI stain is shown as **blue. Bars:** 100 μm **(A and C)**; 50 μm **(E to G)**; 20 μm **(B and D)**. DAPI = 4,6-diamino-2-phyenylindole; MHC = myosin heavy chain; other abbreviations as in Figure 1.

results. Our findings demonstrated that transplantation of hCDCs with bFGF treatment combined the advantages of cardiomyocyte repopulation and stable vascular network formation, resulting in synergistically improved cell therapy efficiency.

Local delivery of combination of growth and survival factor(s), such as insulin-like growth factor 1, on scaffold in cardiac muscles has been shown to improve donor cell survival and enhance tissue repair (21,22). Resident hCDCs may also require joint effects of multiple factors that modulate cell proliferation and differentiation in response to injury. Clinical trials of single protein infusion (23) in human heart disease have shown that the efficacy was not significant in the long term. It is possible that the recombinant protein infused could be rapidly diffused in situ or a combinatorial protein release may be required to achieve the desired degree of angiogenesis in the absence of cell transfer (24). Previous mouse experiments also supported the beneficial effect of bFGF-releasing hydrogel transplantation in the current study, demonstrating that bFGF could be slowly released over time to promote neovascularization initially in situ, and its biological effect was completely terminated as a consequence of hydrogel biodegradation in vivo within 3 weeks after implantation (9).

The less synergistic improvement in animals receiving hBMC injection combined with bFGF than those in hCDC transplants with bFGF was unexpected. Experimental studies in animals suggested that transplantation of BMCs in myocardial infarction could prevent LV remodeling and attenuate the infarct size, mainly through Akt-mediated paracrine effects, despite minimal myocyte regeneration (25). Our results suggested that controlled release of bFGF itself might stimulate these paracrine effectors on host myocardium and showed no additive effects when hBMCs were transplanted.

The cell tracking system using iron-oxide labeling has been reported to be useful to serially monitor the transplanted cells in vivo. However, iron-positive cells may not directly reflect surviving cells, but they are likely to detect the dead cells colocalized with phagocytic macrophages in the host myocardium (26). At least, our results suggested that direct cell injection alone might not be sufficient to achieve efficient myocyte regeneration.

Although our results are limited in the experimental setting of human-pig chimera transplantation, the host animals were immunosuppressed with a dose of cyclosporine A as reported previously (13). Our findings demonstrate a previously undescribed therapeutic efficacy that a combination of bFGF with hCDCs can induce functionally stable microvascular networks to support efficient donor cell engraftment and differentiation. This novel strategy may potentially enhance the cell therapy practically needed to treat patients with heart failure.

Acknowledgments

The authors thank N. J. Brand (Imperial College London) and Y. Kato for kind gifts of plasmids and hBMCs, and J. Kawabe, M. Nakata, Y. Kimura, M. Kuramoto, A. Kosugi, and M. Nishikawa for technical assistance.

Reprint requests and correspondence: Dr. Hidemasa Oh or Dr. Hiroaki Matsubara, Department of Experimental Therapeutics, Translational Research Center, Kyoto University Hospital, Kyoto 606-8507, Japan. E-mail: hidemasa@kuhp.kyoto-u.ac.jp or matsubah@koto.kpu-m.ac.jp.

REFERENCES

1. Murry CE, Field LJ, Menasche P. Cell-based cardiac repair: reflections at the 10-year point. Circulation 2005;112:3174–83.
2. Messina E, De Angelis L, Frati G, et al. Isolation and expansion of adult cardiac stem cells from human and murine heart. Circ Res 2004;95:911–21.
3. Tateishi K, Ashihara E, Honsho S, et al. Human cardiac stem cells exhibit mesenchymal features and are maintained through Akt/GSK-3beta signaling. Biochem Biophys Res Commun 2007;352:635–41.
4. Smith RR, Barile L, Cho HC, et al. Regenerative potential of cardiosphere-derived cells expanded from percutaneous endomyocardial biopsy specimens. Circulation 2007;115:896–908.
5. Bearzi C, Rota M, Hosoda T, et al. Human cardiac stem cells. Proc Natl Acad Sci U S A 2007;104:14068–73.
6. Rosenblatt-Velin N, Lepore MG, Cartoni C, Beermann F, Pedrazzini T. FGF-2 controls the differentiation of resident cardiac precursors into functional cardiomyocytes. J Clin Invest 2005;115:1724–33.
7. Tateishi K, Ashihara E, Takehara N, et al. Clonally amplified cardiac stem cells are regulated by Sca-1 signaling for efficient cardiovascular regeneration. J Cell Sci 2007;120:1791–800.
8. Tabata Y, Nagano A, Muniruzzaman M, Ikada Y. In vitro sorption and desorption of basic fibroblast growth factor from biodegradable hydrogels. Biomaterials 1998;19:1781–9.
9. Tabata Y, Ikada Y. Vascularization effect of basic fibroblast growth factor released from gelatin hydrogels with different biodegradabilities. Biomaterials 1999;20:2169–75.
10. Marui A, Tabata Y, Kojima S, et al. A novel approach to therapeutic angiogenesis for patients with critical limb ischemia by sustained release of basic fibroblast growth factor using biodegradable gelatin hydrogel: an initial report of the phase I-IIa study. Circ J 2007;71:1181–6.
11. Tsutsumi S, Shimazu A, Miyazaki K, et al. Retention of multilineage differentiation potential of mesenchymal cells during proliferation in response to FGF. Biochem Biophys Res Commun 2001;288:413–9.
12. Kajiwara H, Hamada T, Ichikawa Y, Ishi M, Yamazaki I. Experience with expanded polytetrafluoroethylene (ePTFE Gore-Tex) surgical membrane for coronary artery grafting: does ePTFE surgical membrane predispose to postoperative mediastinitis? Artif Organs 2004;28:840–5.
13. Kim BO, Tian H, Prasongsukarn K, et al. Cell transplantation improves ventricular function after a myocardial infarction: a preclinical study of human unrestricted somatic stem cells in a porcine model. Circulation 2005;112:I96–104.
14. Bhavsar PK, Brand NJ, Yacoub MH, Barton PJ. Isolation and characterization of the human cardiac troponin I gene (TNNI3). Genomics 1996;35:11–23.
15. Kaneko T, Tanaka H, Oyamada M, Kawata S, Takamatsu T. Three distinct types of Ca(2+) waves in Langendorff-perfused rat heart revealed by real-time confocal microscopy. Circ Res 2000;86:1093–9.
16. Wollensak G, Green WR. Analysis of sex-mismatched human corneal transplants by fluorescence in situ hybridization of the sex-chromosomes. Exp Eye Res 1999;68:341–6.
17. Amado LC, Saliaris AP, Schuleri KH, et al. Cardiac repair with intramyocardial injection of allogeneic mesenchymal stem cells after myocardial infarction. Proc Natl Acad Sci U S A 2005;102:11474–9.
18. Kraitchman DL, Heldman AW, Atalar E, et al. In vivo magnetic resonance imaging of mesenchymal stem cells in myocardial infarction. Circulation 2003;107:2290–3.
19. Hagendorff A, Werner A, Pfeiffer D, Becher H. Estimation of vasodilator response by analysis of Doppler intensity kinetics with myocardial contrast echocardiography using an intravenous standardized bolus administration. Eur J Echocardiogr 2004;5:272–83.
20. Modesto KM, Cauduro S, Dispenzieri A, et al. Two-dimensional acoustic pattern derived strain parameters closely correlate with one-dimensional tissue Doppler derived strain measurements. Eur J Echocardiogr 2006;7:315–21.
21. Davis ME, Hsieh PC, Takahashi T, et al. Local myocardial insulin-like growth factor 1 (IGF-1) delivery with biotinylated peptide nanofibers improves cell therapy for myocardial infarction. Proc Natl Acad Sci U S A 2006;103:8155–60.
22. Laflamme MA, Chen KY, Naumova AV, et al. Cardiomyocytes derived from human embryonic stem cells in pro-survival factors enhance function of infarcted rat hearts. Nat Biotechnol 2007;25:1015–24.
23. Simons M, Annex BH, Laham RJ, et al. Pharmacological treatment of coronary artery disease with recombinant fibroblast growth factor-2: double-blind, randomized, controlled clinical trial. Circulation 2002;105:788–93.
24. Lu H, Xu X, Zhang M, et al. Combinatorial protein therapy of angiogenic and arteriogenic factors remarkably improves collaterogenesis and cardiac function in pigs. Proc Natl Acad Sci U S A 2007;104:12140–5.
25. Noiseux N, Gnecchi M, Lopez-Ilasaca M, et al. Mesenchymal stem cells overexpressing Akt dramatically repair infarcted myocardium and improve cardiac function despite infrequent cellular fusion or differentiation. Mol Ther 2006;14:840–50.
26. Amsalem Y, Mardor Y, Feinberg MS, et al. Iron-oxide labeling and outcome of transplanted mesenchymal stem cells in the infarcted myocardium. Circulation 2007;116:I38–45.

Key Words: cell therapy ▪ bFGF ▪ gelatin hydrogel ▪ heart failure ▪ myocardial infarction.

APPENDIX

For a discussion of the isolation and characterization of hCDCs, Supplemental Figures 1 and 2, and a Supplemental Table, please see the online version of this article.

Am J Physiol Heart Circ Physiol 295: H2512–H2521, 2008.
First published October 31, 2008; doi:10.1152/ajpheart.00233.2008.

Downregulation of Dicer expression by serum withdrawal sensitizes human endothelial cells to apoptosis

Satoshi Asada,[1,2] Tomosaburo Takahashi,[1,2] Koji Isodono,[1,2] Atsuo Adachi,[1,2] Hiroko Imoto,[1,2] Takehiro Ogata,[2] Tomomi Ueyama,[2] Hiroaki Matsubara,[1,2] and Hidemasa Oh[2]

[1]*Department of Cardiovascular Medicine, Kyoto Prefectural University of Medicine, and* [2]*Department of Experimental Therapeutics, Translational Research Center, Kyoto University Hospital, Kyoto, Japan*

Submitted 4 March 2008; accepted in final form 27 October 2008

Asada S, Takahashi T, Isodono K, Adachi A, Imoto H, Ogata T, Ueyama T, Matsubara H, Oh H. Downregulation of Dicer expression by serum withdrawal sensitizes human endothelial cells to apoptosis. *Am J Physiol Heart Circ Physiol* 295: H2512–H2521, 2008. First published October 31, 2008; doi:10.1152/ajpheart.00233.2008.—Although the modulated expression of Dicer is documented upon neoplastic transformation, little is known of the regulation of Dicer expression by environmental stimuli and its roles in the regulation of cellular functions in primary cells. In this study, we found that Dicer expression was downregulated upon serum withdrawal in human umbilical vein endothelial cells (HUVECs). Serum withdrawal induced a time-dependent repression of Dicer expression, which was specifically rescued by vascular endothelial cell growth factor or sphingosine-1-phosphate. When Dicer expression was silenced by short-hairpin RNA against Dicer, the cells were more prone to apoptosis under serum withdrawal, whereas the rate of apoptosis was comparable with control cells in the serum-containing condition. Real-time PCR-based gene expression profiling identified several genes, the expression of which was modulated by Dicer silencing, including adhesion and matrix-related molecules, caspase-3, and nitric oxide synthase 3 (NOS3). Dicer silencing markedly impaired migratory functions without affecting cell adhesion and repressed phosphorylation of focal adhesion kinase and proline-rich tyrosine kinase 2 in adherent HUVECs. Dicer knockdown upregulated caspase-3 and downregulated NOS3 expression, and serum withdrawal indeed increased caspase-3 and decreased NOS3 expression. Furthermore, the overexpression of Dicer in HUVECs resulted in a marked reduction in apoptosis upon serum withdrawal and a decreased caspase-3 and increased NOS3 expression. The inhibition of NOS activity by N^{ω}-nitro-L-arginine methyl ester abrogated the effect of Dicer overexpression to rescue the cells from serum withdrawal-induced apoptosis. These results indicated that serum withdrawal decreases Dicer expression, leading to an increased susceptibility to apoptosis through the regulation of caspase-3 and NOS3 expression.

caspase 3; nitric oxide synthase 3

APOPTOSIS IS A PROCESS OF innate cellular death, controlled by complex and diverse molecular mechanisms with considerable cell-type specificity. Apoptosis plays important roles in various aspects of biology from the development to a wide range of diseases such as cancers and cardiovascular diseases. In the vasculature, the integrity of the endothelial lining is essential for vascular homeostasis and for normal organ function, and endothelial cell apoptosis has been implicated not only in normal physiological events such as blood vessel development, homeostasis, and remodeling but also in pathological conditions associated with endothelial dysfunction such as inflammatory and immune disorders, tumor growth, and atherosclerosis (31, 32, 46). Although apoptotic processes are tightly regulated by extracellular factors and intracellular signalings, the precise molecular mechanisms governing endothelial cell apoptosis have not been fully elucidated, and understanding the regulation of apoptosis is of great importance for the advancement of endothelial biology and for developing novel therapeutic strategies.

Dicer is a cytoplasmic RNase III enzyme, which cleaves microRNA (miRNA) and small-interfering RNA (siRNA) precursors into about 22 nucleotide species (17, 45). The function of Dicer in the biogenesis of small RNAs is central to miRNA and RNA interference pathways, and Dicer presumably mediates the processing of all miRNAs and endogenous siRNAs. In their short mature forms, miRNA and siRNA function to regulate gene expression through the posttranscriptional regulation of protein-coding gene expression (2, 9). In mammals, most miRNAs mediate translational repression by forming an imperfect base pairing to 3′ untranslated regions of target mRNAs, whereas siRNAs induce target mRNA degradation through establishing a perfect pairing, which can occur throughout the message. The human genome encodes hundreds of miRNAs, which are estimated to regulate the expression of as many as 30% of protein-coding genes (2). Dicer transcript is expressed from the embryonic through adult stages of development and is also present in a wide variety of adult organs, whereas the expression levels vary between organs (50).

In addition to being important in miRNA and RNA interference pathways, Dicer is shown to be crucial in controlling cell cycle checkpoints, especially in response to mutagenic stress (5, 41), proper structuring of centromeric heterochromatin (13), and organization of the germ line (36). Dicer null mutation in mice shows embryonic lethal phenotype at E 7.5 (4), and Dicer-deficient embryonic stem cells are defective in differentiation both in vivo and in vitro (35). Although these results indicate the important role of Dicer in development and stem cell maintenance, Dicer could have functions specific for differentiated cell types. For example, a specific deletion of Dicer in T-cell lineage results in aberrant T-cell differentiation and cytokine production, whereas the transcriptional gene silencing during CD4/8 differentiation is not perturbed (33). The inactivation of Dicer activity in skin progenitors results in an abnormal epithelium morphogenesis (1), and Dicer inactivation in lung epithelium leads to dramatic branching defects

Address for reprint requests and other correspondence: T. Takahashi, Dept. of Cardiovascular Medicine, Kyoto Prefectural Univ. of Medicine, 465 Kajii-cho Kawaramachi-Hirokoji, Kamigyo-ku, Kyoto 602-8566, Japan (e-mail: ttaka@koto.kpu-m.ac.jp).

The costs of publication of this article were defrayed in part by the payment of page charges. The article must therefore be hereby marked "*advertisement*" in accordance with 18 U.S.C. Section 1734 solely to indicate this fact.

in lung (19). Recent reports identified Dicer as an important component to control endothelial functions related to angiogenesis such as proliferation, migration, and morphological differentiation into capillary-like structure (26, 47, 50). However, little is known about the regulation of Dicer expression by environmental stimuli and its roles in the regulation of cellular functions in endothelial cells.

Here, to uncover functions of Dicer in endothelial biology, we first explored the condition that modulated the expression of Dicer in human umbilical vein endothelial cells (HUVECs) and found that serum withdrawal induced the reduction in Dicer expression. Silencing Dicer expression by short-hairpin (sh)RNA led to an increased susceptibility of endothelial cells to apoptosis, and an overexpression of Dicer protected cells from apoptosis induced by serum deprivation. Furthermore, caspase-3 and nitric oxide synthase 3 (NOS3) expression was modulated by Dicer expression. These results indicated that a regulation of Dicer expression involves an apoptotic response of endothelial cells to serum withdrawal.

MATERIALS AND METHODS

Cell culture. HUVECs (Clonetics) were cultured in RPMI-1640 medium supplemented with 20% fetal bovine serum (FBS), 40 μg/ml endothelial cell growth supplement (BD Biosciences), heparin, and penicillin-streptomycin on 0.5% gelatin-coated dishes and used between *passages* 2 and 5 for all experiments as described previously (42). Human foreskin fibroblasts (Riken Cell Bank) were cultured in DMEM supplemented with 10% FBS. To induce apoptosis, confluent HUVECs were cultured in the medium without serum and endothelial cell growth supplement for the indicated period of time.

Kinetic real-time RT-PCR. cDNA was synthesized and analyzed by kinetic real-time PCR with the ABI Prism 7700 Sequence Detector system (Applied Biosystems) and Platinum SYBR Green qPCR SuperMix (Invitrogen) as described previously (24, 37). Human β-tubulin was used for normalization, and the comparative threshold method was used to assess the relative abundance of the targets. The primers used were Dicer-f, TGGGTCCTTTCTTTGGACTG; Dicer-r, CTGGTTTGCAGAGTTGACCA; caspase-3-f, TGGAATTGATGCGTGATGTT; caspase-3-r, GGCAGGCCTGAATAATGAAA; NOS3-f, ACCCTCACCGCTACAACATC; NOS3-r, GCTCATTCTCCAGGTGCTTC; β-tubulin-f, CTCTGAAGCTGACCACACCA; and β-tubulin-r, GCCAGGCATAAAGAAATGGA.

Immunoblot analysis. Cell lysates containing equal amounts of protein were electrophoresed on SDS-polyacrylamide gels and transferred to polyvinylidene difluoride membranes (Millipore). Blots were immunoblotted with the primary antibody against Dicer (Abcam), phospho-proline-rich tyrosine kinase 2 (PYK2) (Biosource), PYK2 (BD Biosciences), phospho-focal adhesion kinase (FAK), FAK, phospho-Src, Src, phospho-ERK, ERK, phospho-p38-MAPK, p38-MAPK, phospho-JNK, JNK, caspase-3 (Cell Signaling), NOS3 (Santa Cruz), or GAPDH (Chemicon), and horseradish peroxidase-conjugated anti-mouse or -rabbit IgG as a secondary antibody, followed by enhanced chemiluminescence (GE Healthcare) (24, 37).

Short-hairpin RNA interference. Short-interfering RNA constructs (shRNA) was made with RNAi-Ready pSIREN-RetroQ vector (Clontech). To knockdown endogenous Dicer expression, we used the published sequences of siRNA, which is shown to specifically silence Dicer expression in various types of cells including HUVECs (7, 16, 47). Sense (ACATCAAGGTGCTAATAGA) and antisense oligonucleotides corresponding to nucleotides 3581–3599 of the human Dicer cDNA was cloned into pSIREN-RetroQ vector with the hairpin loop sequence of TTCAAGAGA, according to the manufacturer's instruction. pSIREN-RetroQ control Si vector (Clontech) was used as a control.

Retrovirus production and infection. GP2-293 cells (Clontech) were cotransfected with envelop vector pVSV-G and each pSIREN-RetroQ vector using FuGENE6 (Roche) (37). After 24 h, the medium was exchanged, and the medium containing the emerging retrovirus was harvested 48 h after transfection, filtered, and then incubated with HUVECs in the presence of 6 μg/ml polybrene for 6 h. Twenty-four hours later, the retroviral supernatant was harvested for a second time, and HUVECs were infected again (30). HUVECs were then selected with 0.5 μg/ml puromycin for 3 days. The transfection efficiency for HUVECs was almost 100%, when assessed with enhanced green fluorescent protein-expressing retrovirus.

Northern blot analysis. Total RNA samples were electrophoresed on denaturing 15% polyacrylamide gels and electroblotted onto GeneScreen Plus membranes (Perkin-Elmer) as described previously (37). The membranes were UV-cross-linked, baked, and hybridized with ^{32}P end-labeled oligonucleotide DNA probes in ULTRAhyb-Oligo (Ambion). After a washing, hybridization signals were detected using the Bio-imaging analyzer system BAS5000 (Fuji Film). Human U6 was used as an internal control.

Quantitative RT-PCR for miRNA. Quantitative real-time PCR for miRNA was carried out using TaqMan MicroRNA assays (Applied Biosystems) with ABI Prism 7700 Sequence Detector system (Applied Biosystems) according to the manufacturer's instruction. These assays only detect mature miRNAs but not primary or precursor forms of miRNAs. For normalization, 18s rRNA was used, and the comparative threshold method was used to assess the relative abundance of the targets.

Transferase-mediated biotinylated UTP nick-end labeling assay. Apoptotic cells were detected by in situ terminal deoxynucleotidyl transferase-mediated biotinylated UTP nick-end labeling (TUNEL) assay using ApopTag Red In Situ Apoptosis Detection Kit (Chemicon) (48). In brief, HUVECs cultured on collagen type I-coated two-well culture slide (BD Biosciences) were fixed, and fragmented DNA was labeled with digoxigenin-labeled deoxyNTP in the presence of terminal deoxynucleotidyl transferase enzyme, followed by staining with rhodamine-conjugate anti-digoxigenin antibody. Cells were nuclear stained with 4′,6′-diamidino-2-phenylindole (DAPI, Dojindo) and mounted using PermaFluor Mountant Medium (Thermo Scientific). The TUNEL-positive and total nuclei were counted under a fluorescent microscope (IX71, Olympus) in five view fields per well.

Gene expression analysis by PCR array. RT^2 Profiler PCR Array (SuperArray Bioscience) was used to examine the expression pattern of genes involved in endothelial cell biology. The array consists of 84 genes involved in endothelial cell biology as well as five housekeeping genes, and an analysis was carried out according to the manufacturer's instruction.

Adhesion assay. Four-hundred microliters of cell suspension containing 4×10^4 cells in serum-free medium was placed in each well of 24-well plates coated with 0.5% gelatin or 1 μg/ml human fibronectin (BD Biosciences). After the cells were allowed to adhere for 30 min, loosely adherent or unbound cells were removed by washing the wells with PBS, and the adherent cells were fixed and stained with DAPI. The nuclei of adherent cells were counted under the fluorescent microscope in five view fields per well.

Migration assay. Transwell migration was analyzed in a modified Boyden chamber assay using BioCoat 24-multiwell insert system (BD Biosciences) with a 3-μm pore-size PET membrane coated with human fibronectin. HUVECs (1.0×10^5), suspended in RPMI 1640 medium containing 1% FBS, were added to the upper compartment of the membrane. Culture medium containing 10 ng/ml vascular endothelial cell growth factor (VEGF) was used as a chemoattractant and placed in the lower compartment. After incubation for 4 h, the membranes were fixed and stained with DAPI (Dojindo), and the cells attached to the bottom side of the membrane were counted under the microscope (IX71, Olympus).

Lateral migration was assessed by a wound healing assay (42). Confluent monolayers of HUVECs were wounded with a pipette tip.

Twenty hours later, wound closure was quantified by the percent change in the wound area and averaged for three locations per well from a triplicate set of samples for each experimental condition.

Transfection. For an overexpression of Dicer, HUVECs were grown to 60% to 70% confluence and transfected with pDH105 Dicer expression vector (a kind gift from Jason Myers, Stanford University) using Lipofectamine LTX Reagent and PLUS Reagent (Invitrogen). HUVECs were incubated with DNA-lipofectamine LTX complexes at 37°C for 2 h in the absence of serum, followed by a recovery in the presence of 20% FBS. pMSCV-puro GFP vector was used as a control, and maximal levels of protein expression were observed between 48 and 72 h.

Statistical analysis. All experiments were performed at least three times. Data were expressed as means ± SE and analyzed by unpaired Student's *t*-test for comparisons between two groups or one-way ANOVA with post hoc analysis for multiple comparisons. A value of $P < 0.05$ was considered statistically significant.

RESULTS

Serum withdrawal leads to the reduction in Dicer expression in endothelial cells. Although Dicer is shown to be involved in several important functions of endothelial cells, little is known about the regulation of Dicer expression in endothelial cells. Therefore, we first explored the condition that modulated the expression of Dicer in HUVECs and found that serum withdrawal induced a significant reduction in Dicer mRNA and protein expression (Fig. 1*A*). Dicer was expressed in HUVECs, and upon serum withdrawal, Dicer expression was reduced in a time-dependent manner (Fig. 1*A*). The reduction in Dicer expression was readily detectable 12 h after serum withdrawal, and Dicer expression was gradually decreased up to 48 h after serum withdrawal, whereas the expression of GAPDH remained unchanged. To characterize the serum components responsible for maintaining Dicer expression in HUVECs, the cells were cultured with VEGF, basic fibroblast growth factor (bFGF), sphingosine-1-phosphate (S1P), or lysophosphatidic acid (LPA) in serum-free medium for 48 h, and the Dicer expression was analyzed. As shown in Fig. 1*B*, VEGF and S1P, but not bFGF and LPA, rescued serum withdrawal-induced downregulation of Dicer expression. We also tested whether serum withdrawal affected Dicer expression in human fibroblasts. In fibroblasts, serum withdrawal also reduced Dicer expression (Fig. 1*C*). These results indicated that upon serum withdrawal, Dicer expression is downregulated in HUVECs, and VEGF and S1P could play a role to maintain Dicer expression.

Silencing Dicer expression impairs miRNAs processing. In mice and humans, Dicer is encoded by a single locus, the protein product of which could account for all Dicer activity. To investigate the functional significance of Dicer expression in endothelial cells, we generated a retrovirus vector expressing shRNA against Dicer. Upon infection with this Dicer shRNA-expressing retrovirus, Dicer expression in HUVECs was downregulated by ~70% in mRNA expression (Fig. 2*A*), and the protein expression of Dicer was barely undetectable in immunoblot analysis (Fig. 2*B*). The expression of Dicer mRNA and protein in cells infected with retrovirus expressing control shRNA was comparable with that in naïve noninfected cells (Fig. 2, *A* and *B*).

As Dicer is known to be critical for pre-miRNA processing, we examined the expression of let-7a and miR-221, two miRNAs abundantly expressed in HUVECs (26, 40). In noninfected naïve cells and control shRNA-expressing cells, Northern blot analysis revealed that these two miRNAs were

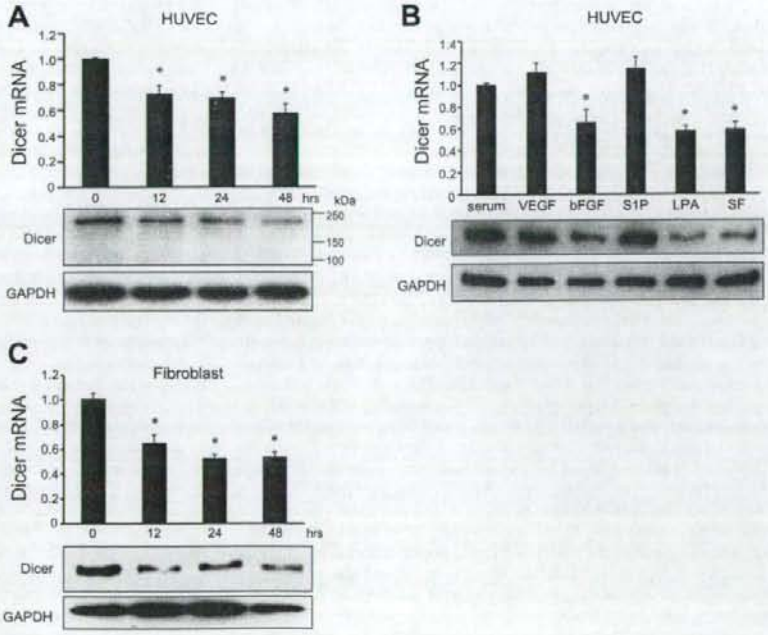

Fig. 1. Serum withdrawal decreases Dicer expression in endothelial cells. Naïve human umbilical vein endothelial cells (HUVECs) or human fibroblasts were grown to be confluent in complete medium and then replaced with serum-free (SF) medium for the indicated periods of time. *A*: mRNA expression of Dicer in HUVECs was analyzed by kinetic real-time PCR. The results from at least 3 independent trials were expressed relative to the level of β-tubulin and plotted as percentages of the control. $*P < 0.05$ vs. control. Protein expression of Dicer was examined by immunoblot analysis. The membranes were reprobed with anti-GAPDH antibody. *B*: confluent HUVECs were cultured with or without 20% FBS, 10 ng/ml VEGF, 10 ng/ml basic fibroblast growth factor (bFGF), 10 μM sphingosine-1-phosphate (S1P), or 10 μM lysophosphatidic acid (LPA) for 48 h, and mRNA and protein expression of Dicer was analyzed. $*P < 0.05$ vs. FBS. *C*: human fibroblasts were cultured in serum-free medium for the indicated periods of time, and mRNA and protein expression of Dicer was analyzed. $*P < 0.05$ vs. control. Blots shown represent 1 of at least 3 independent trials that gave nearly identical results.

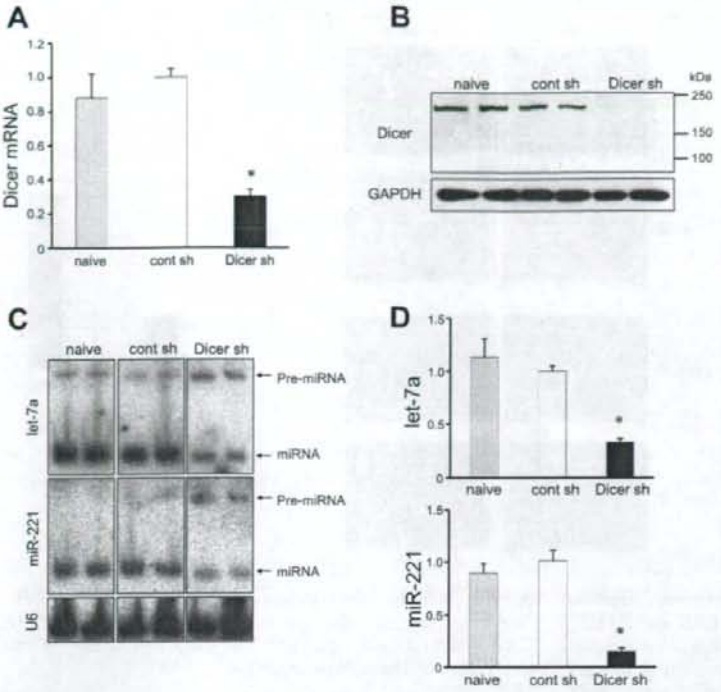

Fig. 2. Silencing Dicer expression impairs microRNA (miRNA) processing. Cells were infected or not infected with retrovirus expressing control or Dicer short-hairpin (sh)RNA. *A*: Dicer mRNA expression was examined by kinetic real-time PCR in naïve, control shRNA (Cont SH) or Dicer shRNA HUVECs. The results were expressed as relative expression to β-tubulin and plotted as ratios of the control shRNA HUVECs. $^*P < 0.05$ vs. control shRNA cells. *B*: immunoblot analysis was performed to analyze Dicer protein expression. *C*: expression of let-7a and miR-221 was analyzed by Northern blot analysis, and U6 was used as a loading control. *D*: quantitative real-time PCR for miRNA was performed for let-7a and miR-221 expression, and the results were expressed as ratios of the control shRNA HUVECs. $^*P < 0.05$ vs. control shRNA cells.

detectable as strong and faster migrating bands for their mature forms and as faint and slower migrating bands for their precursors (Fig. 2*C*). Dicer knockdown led to a significant decrease in the accumulation of mature miRNAs and an increase in the precursors of these miRNAs (Fig. 2*C*). The reduction in the accumulation of mature miRNAs was also verified by real-time PCR for miRNA, which only detects mature forms of miRNAs (Fig. 2*D*). These results indicated that Dicer is indispensable for miRNA processing from the pre-miRNA to mature forms in endothelial cells, and Dicer knockdown compromises the maturation of miRNAs, resulting in a reduced expression of mature miRNAs.

Silencing Dicer expression results in susceptibility of endothelial cells to apoptosis in response to serum deprivation. As the withdrawal of survival factors has been demonstrated to cause apoptosis of endothelial cells and as serum withdrawal reduced the expression of Dicer (Fig. 1), the effect of silencing Dicer expression on apoptosis in response to serum withdrawal was examined. When Dicer expression was silenced by retrovirus-mediated expression of shRNA, the percentage of apoptotic cells was markedly increased compared with control shRNA cells in a serum-starved condition, whereas the proportion of apoptotic cells remained unchanged in a serum-containing condition (Fig. 3, *A* and *B*). These results suggested that a reduced expression of Dicer conferred the cells susceptibility to apoptosis under the stress of serum deprivation.

Dicer silencing modulates expression of multiple genes including caspase 3 and NOS3. To explore the effect of reduced expression of Dicer on gene expression involved in endothelial biology, we used real-time PCR-based gene expression profiling to compare the gene expression profiles in control and Dicer shRNA-expressing cells and identified several genes, the expression of which was significantly modulated by Dicer silencing (Fig. 4*A*). Among them, a modulated expression of NOS3 and caspase-3 was further verified at the mRNA level by real-time kinetic PCR with other sets of primers than those used in a PCR array and at the protein level by immunoblotting (Fig. 4*B*). Dicer silencing induced a significant increase in caspase-3 expression and a decrease in NOS3 expression (Fig. 4*B*). These results indicated that a reduced expression of Dicer affects the expression of multiple genes involved in endothelial biology and suggested that an altered expression of caspase-3 and NOS3 was involved in the susceptibility to apoptosis of endothelial cells.

Dicer silencing impairs migratory functions and adhesion-mediated phosphorylation of FAK and PYK2. As the modulated expression of adhesion and extracellular matrix-related molecules was observed in gene expression profiling (Fig. 4*A*), the adhesive and migratory functions of HUVECs were analyzed. An adhesion assay revealed that the adhesiveness of cells to gelatin- or fibronectin-coated dishes was not significantly altered by Dicer silencing (Fig. 5*A*). However, the migratory functions assessed by a Boyden chamber assay and wound healing assay were largely impaired in Dicer knockdown cells (Fig. 5, *B* and *C*). Furthermore, the phosphorylation of FAK and PYK2 was diminished by Dicer knockdown in adherent HUVECs, whereas the activation of Src, Akt, and MAPKs such as ERK, p38 MAPK, and JNK was not affected

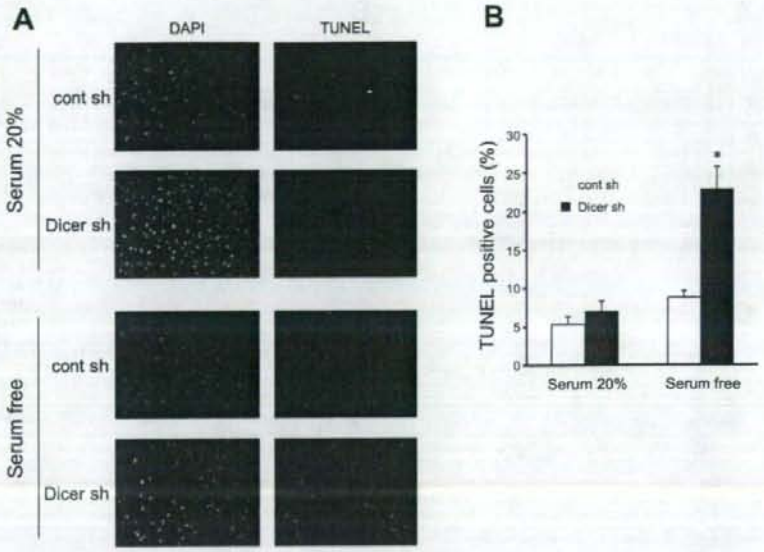

Fig. 3. Silencing Dicer expression sensitizes endothelial cells to apoptosis in response to serum withdrawal. Control shRNA and Dicer shRNA HUVECs were cultured in the presence or absence of serum for 12 h. *A*: transferase-mediated biotinylated UTP nick-end labeling (TUNEL) staining was carried out to examine apoptosis in control shRNA and Dicer shRNA HUVECs. DAPI, 4′,6′-diamidino-2-phenylindole. *B*: TUNEL-positive and total nuclei in control shRNA and Dicer shRNA HUVECs were quantified, and the proportion of TUNEL-positive cells was plotted. $^*P < 0.05$ vs. control shRNA cells.

(Fig. 5*D*). Thus Dicer silencing impaired migratory functions and adhesion-mediated phosphorylation of FAK and PYK2.

Serum withdrawal results in an increase in caspase-3 expression and a decrease in NOS3 expression. In the next sets of experiments, it was analyzed whether serum withdrawal, which decreased Dicer expression (Fig. 1), modulated caspase-3 and NOS3 expression in endothelial cells. As shown in Fig. 6, serum starvation indeed increased caspase-3 expression and decreased NOS3 expression in a time-dependent manner. These results suggested that a reduction in endogenous Dicer expression in response to serum deprivation was involved in the regulation of caspase-3 and NOS3 expression.

Overexpression of Dicer protects endothelial cells from apoptosis induced by serum withdrawal. To analyze the functional significance of the reduced expression of Dicer in response to serum withdrawal, Dicer was overexpressed in endothelial cells, and the apoptotic response to serum withdrawal was assessed. Cells overexpressing Dicer were resistant to apoptosis in response to serum deprivation, and the rate of apoptosis in the serum-deprived condition was reduced to the level comparable with the serum-containing condition in Dicer-overexpressing cells (Fig. 7*A*). These results clearly indicated that the expression of Dicer regulates the susceptibility of endothelial cells to apoptosis in response to serum withdrawal. Furthermore, Dicer overexpression reduced caspase-3 expression and enhanced the expression of NOS3, suggesting the regulatory role of the Dicer expression level in caspase-3 and NOS3 expression in endothelial cells.

To examine the role of the enhanced expression of NOS3 in Dicer-overexpressing cells in protecting from apoptosis, the effect of N^{ω}-nitro-L-arginine methyl ester (L-NAME), a NOS inhibitor, on the reduced apoptotic response by Dicer overexpression was analyzed. L-NAME treatment significantly blocked the effect of Dicer overexpression to rescue the cell from apoptosis induced by serum withdrawal (Fig. 7*C*), implying that the enhanced expression of NOS3 by Dicer overexpression plays an important role in the protective effect of Dicer expression.

DISCUSSION

Although the roles of Dicer in several important cellular functions are reported, most of these results are based on the experiments in which Dicer expression is modulated with a genetic modification in mice or a gene silencing with siRNA in cells, and little is known whether Dicer expression is regulated in certain circumstances. An aberrant expression of Dicer has been most demonstrated in several neoplasms. An increased expression of Dicer is reported in Burkitt's lymphoma-derived cell line EB-3 (22) and prostate adenocarcinomas (8). In the latter case, Dicer expression is shown to correlate with aggressive clinical features. On the other hand, in non-small lung carcinomas, the reduced expression of Dicer is associated with shorter postoperative survival (21). Expression profiling of miRNA revealed a global repression of miRNA expression in cancer samples and cell lines (15, 29). A recent report has shown that Dicer knockdown results in an increased colony formation in culture and an increased tumor growth in vivo only in cells that are already transformed, whereas a reduction in Dicer leads to slow growth kinetics in primary cells (27). These results indicate that the effect of the modulated expression of Dicer is cell-type and context dependent and imply the importance of elucidating the conditions that alter the expression of Dicer and its consequences in specialized cells. In endothelial cells, it has been reported that Dicer is constitutively expressed (26, 47), and its expression is not altered by a stimulation with VEGF (47). In this study, we found that serum withdrawal, a stress of trophic factor deprivation, markedly repressed Dicer expression in HUVECs. We also demonstrated that VEGF and S1P, but not bFGF and LPA, rescued the